DOI: 10.1002/cne.24678

Received: 22 December 2018

### RESEARCH ARTICLE



# Mushroom bodies in crustaceans: Insect-like organization in the caridid shrimp Lebbeus groenlandicus

Accepted: 28 February 2019

Marcel E. Savre<sup>1</sup> | Nicholas J. Strausfeld<sup>2</sup>

#### Correspondence

Nicholas J. Strausfeld, University of Arizona, Department of Neuroscience, GS 611, University of Arizona, Tucson, AZ 85721. Email: flvbrain@email.arizona.edu

#### Funding information

National Science Foundation Grant/Award Number: 1754798

#### Abstract

Paired centers in the forebrain of insects, called the mushroom bodies, have become the most investigated brain region of any invertebrate due to novel genetic strategies that relate unique morphological attributes of these centers to their functional roles in learning and memory. Mushroom bodies possessing all the morphological attributes of those in dicondylic insects have been identified in mantis shrimps, basal hoplocarid crustaceans that are sister to Eumalacostraca, the most species-rich group of Crustacea. However, unless other examples of mushroom bodies can be identified in Eumalacostraca, the possibility is that mushroom body-like centers may have undergone convergent evolution in Hoplocarida and are unique to this crustacean lineage. Here, we provide evidence that speaks against convergent evolution, describing in detail the paired mushroom bodies in the lateral protocerebrum of a decapod crustacean, Lebbeus groenlandicus, a species belonging to the infraorder Caridea, an ancient lineage of Eumalacostraca.

#### **KEYWORDS**

evolution, hemiellipsoid body, homology, mushroom body, Pancrustacea, RRID:AB\_1157911, RRID:AB\_1566510, RRID:AB\_301787, RRID:AB\_477,019, RRID:AB\_528479, RRID: AB\_572263, RRID:AB\_572268

#### 1 | INTRODUCTION

Olfactory centers in the brains of crustaceans consist of the paired deutocerebral olfactory lobes, supplied by the antennules (first antennae), the relay neurons of which provide long axons that reach the brain's lateral protocerebrum. In most crustacean lineages, olfactory relay neurons terminate there in a domed or cupula-like neuropil traditionally referred to as the hemiellipsoid body (Bellonci, 1882). Observations of Stomatopoda, hoplocarid crustaceans that are the sister group of Eumalacostraca (Schwentner, Richter, Rogers, & Giribet, 2018), showed that elongated columnar neuropils (the corpo allungato; Bellonci, 1882) extend from the hemiellipsoid body in a manner that in conjunction with the hemiellipsoid body suggested these correspond to the insect mushroom body lobes and calyces. A recent study has confirmed that the mushroom bodies of stomatopods are indeed phenotypic homologues of the paired insect mushroom bodies, sharing all of 13 neuroanatomical traits identified as defining an insect mushroom body (Wolff, Thoen, Marshall, Sayre, & Strausfeld, 2017). Prominent mushroom bodies in insects have been proposed to relate to refined

spatial memory. Mushroom body elaboration in parasitoid Hymenoptera has been attributed not to the evolution of eusociality but to the evolution of olfactory spatial memory that informs the individual about the location and readiness of an intended host to receive the parasitoid's egg (Farris & Schulmeister, 2011). There is a direct relationship between the size of paired mushroom bodies and the ability to remember visual and olfactory cues used in the memory of locations during trap-line foraging (Montgomery, Merrill, & Ott, 2016), and comparisons of solitary bees showed those with foraging experience had the largest mushroom bodies (Withers, Day, Talbot, Dobson, & Wallace, 2008). In the ant Camponotus floridanus, experienced workers achieve about 50% enlargement of the mushroom bodies compared with base-line naïve workers (Gronenberg, Heeren, & Hölldobler, 1996). In crustaceans, the enormous mushroom bodies of mantis shrimps have been suggested to relate to predatory hunting or ambush behaviors that rely on the memory of landmarks as reviewed by Cronin, Caldwell, and Marshall (2006). The prodigious mushroom bodies of pistol shrimps (Wolff et al., 2017), the only group of eusocial crustaceans (Duffy, 1996), are also suggestive of their possessing refined spatial memory. As in parasitoid and

<sup>&</sup>lt;sup>1</sup>Lund Vision Group, Department of Biology, Lund University, Lund, Sweden

<sup>&</sup>lt;sup>2</sup>Department of Neuroscience, School of Mind, Brain and Behavior, University of Arizona, Tucson, Arizona



eusocial hymenopterous insects, the protocerebra of pistol shrimps are dominated by enormous paired mushroom body-like centers characterized by elevated expression of *Drosophila* "learning and memory" proteins and the arrangements of many thousands of parallel fibers emanating from clustered globuli cells (Wolff et al., 2017). Might other species of Crustacea that employ or are likely to employ landmark orientation reveal anatomical features comparable to insect and stomatopod mushroom bodies, and if so, have mushroom bodies evolved once or more than once?

Here, we describe centers that dominate the lateral protocerebral lobes of the caridid shrimp Lebbeus groenlandicus (Figure 1a). Lebbeids are a branch of the super family Alpheoidea, to which also belongs the genus Alpheus, its members including pistol shrimps. L. groenlandicus (Fabricius, 1775), commonly referred to as spiny lebbeid, is an epibenthic decapod crustacean widely distributed across the northern Atlantic and northern Pacific Oceans (Jensen, 1995; Komai, 2015). Individuals of L. groenlandicus inhabit rocky ecologies, which accounts for the infrequent capture of this species using trawl nets. In captivity, individuals exhibit aggressive territorial behavior until territories are established, after which individuals settle. However, although few observations have been made of this species in the wild, reports of a related lebbeid. L. mundus from the northwest Pacific, describe that species as cleaning the mouths of fish that visit it (Jensen, 2006). The body and appendages of L. groenlandicus are brightly and spectacularly patterned into irregular white and orange-pink stripes (Figure 1b), features that suggest it indulges in self-advertisement in a manner typical of eucaridids, such as harlequin shrimps (Stenopodidea) that participate in symbiotic cleaning of fish (Limbaugh, Pederson, & Chase, 1961).

We show here that the lateral protocerebra of L. groenlandicus contain elaborate paired multimodal centers, traditionally referred as the hemiellipsoid bodies, that receive relays from the deutocerebrum's olfactory lobes and lateral antennular neuropils (LAN) as well as from the protocerebrum's optic lobes (Figure 1c). In L. groenlandicus, the organization of these centers departs from the accepted view that hemiellipsoid bodies comprise just 2-3 distinct adjacent or layered territories (see: Stemme, Eickhoff, & Bicker, 2014). As in Stomatopoda, in L. groenlandicus these centers comprise an elaborate large and a smaller calyx, both distinctly stratified, composed of palisades of neurons, the axon-like processes of which converge and then extend proximally from the inner face of each calyx to provide two columnar neuropils. Within the columns, many hundreds of these axon-like processes contribute to orthogonal networks that are intercepted by the arborizations of terminals from other brain areas and the dendritic arbors of output neurons to other protocerebral neuropils, some extending recurrently to the calyces. This organization corresponds neuroanatomically to the ground pattern organization of the mushroom body calyces and lobes of insects and stomatopods (Strausfeld, Sinakevitch, Brown, & Farris, 2009; Wolff et al., 2017). Immunocytology further demonstrates corresponding arrangements of putative inhibitory, modulatory, and dopaminergic neurons as well as upregulated expression of DCO, a protein that in Drosophila mushroom bodies is essential for learning and memory (Skoulakis, Kalderon, & Davis, 1993). While less elaborate than those of stomatopods, the presence of mushroom bodies in L. groenlandicus suggests special memory requirements associated with memory of place and, as in certain other Alpheoidea, possibly reciprocal altruism (Feder, 1966; Limbaugh et al., 1961; Trivers, 1971).

#### 2 | MATERIALS AND METHODS

#### 2.1 | Crustacean species

Adult specimens of *L. groenlandicus* were collected near San Juan Island (Washington) by trawling along the Puget Sound at a depth of up to 80 m (at approximately N48°34.7′, W123°02.8′). Shrimps were transported to shaded outdoor marine tanks that were supplied by constantly circulating seawater. In some cases, shrimps were kept in an incubation room inside filtered tanks maintained at 10°C on a 12-hr light/dark cycle. Ocean water salinity was measured at time of capture and in the laboratory replicated as closely as possible (approx. 35 ppt). Twenty-five animals were collected and maintained at Friday Harbor Research Facilities (University of Washington; Friday Harbor, WA) for immediate immunohistochemistry. Twelve animals were shipped to the Arizona laboratory aquaria for later silver impregnations and additional immunohistochemistry.

## 2.2 | Golgi impregnations

Golgi impregnations, which stochastically define individual neurons, have been employed to resolve fundamental attributes of nerve cell arrangements within and between circumscribed neuropils (Figures 1h, 2 and 3c-i). Animals (n = 6) were immersed in ice and briefly anesthetized. Eyestalk and midbrain tissue were then dissected in cold fixative containing one part 25% glutaraldehyde (Electron Microscopy Sciences; Cat# 16220; Hatfield, PA), five parts 2.5% potassium dichromate (Sigma Aldrich; Cat# 207802; St. Louis, MO), and 10% sucrose, being careful to fully remove the enveloping neural sheath. Following dissection, whole brains were moved to fresh fixative and left overnight in the dark at room temperature (RT). The remainder of the protocol was carried out at RT with preparations left in the dark whenever possible.

The following day, brains were briefly washed in 2.5% potassium dichromate and then transferred to a vial containing 2.5% potassium dichromate with 0.005% osmium tetroxide (Electron Microscopy Sciences; Cat# 19150; Hatfield, PA), and left 12–24 hr. Next, preparations were moved to a fresh solution of 2.5% potassium dichromate and 0.01% osmium tetroxide and again left overnight. Then, tissue was rinsed three times in 2.5% potassium dichromate and quickly transferred twice into fresh solutions of 0.75% silver nitrate (Electron Microscopy Sciences; Cat# 21050; Hatfield, PA) where it was left to incubate 12–24 hr. For double impregnations, the second osmification step was repeated following incubation in silver nitrate. The silver nitrate step was then repeated.

After silver nitrate treatment, tissue was rinsed twice in water and dehydrated through an increasing ethanol series of 50, 70, 90%, and 2  $\times$  100% for 8 min each. Tissue was then transferred into propylene oxide for 15 min and embedded through an increasing Durcupan (Sigma Aldrich; Cat# 44610; St. Louis, MO) series of 25, 50, 75, and 100% Durcupan at 1-hr steps. Blocks were polymerized at 60°C overnight, trimmed, sectioned either frontally or sagittally at 20–40  $\mu m$ , and mounted on slides in Permount mounting medium (Fisher Scientific; Cat# SP15-100; Hampton, NH).

### 2.3 | Bodian staining

Bodian's reduced silver technique (Bodian, 1936) has been used to resolve the neuroarchitectures of and relationships among delineated synaptic neuropils (Figures 1d-f, i-n and 4c-e). Shrimp brains (n = 3) were dissected and fixed in acetic alcohol formalin fixative (AAF; 42.5 mL 80% ethanol, 10 mL 16% paraformaldehyde (PFA), 2.5 mL glacial acetic acid) overnight at RT. Following fixation, whole brains

were dehydrated through a graded ethanol series (as described in Section 2.2), passed through  $\alpha$ -terpineol (Sigma Aldrich; Cat# 432628; St. Louis, MO), into xylenes (15 min for each), and embedded in Paraplast Plus (Sherwood Medical, St. Louis, MO). Blocks were sectioned at 12  $\mu$ m and subsequently processed following Bodian's original method (Bodian, 1936).

Briefly, slides containing the tissue sections were rehydrated through xylenes and ethanol by repeating the dehydration series in

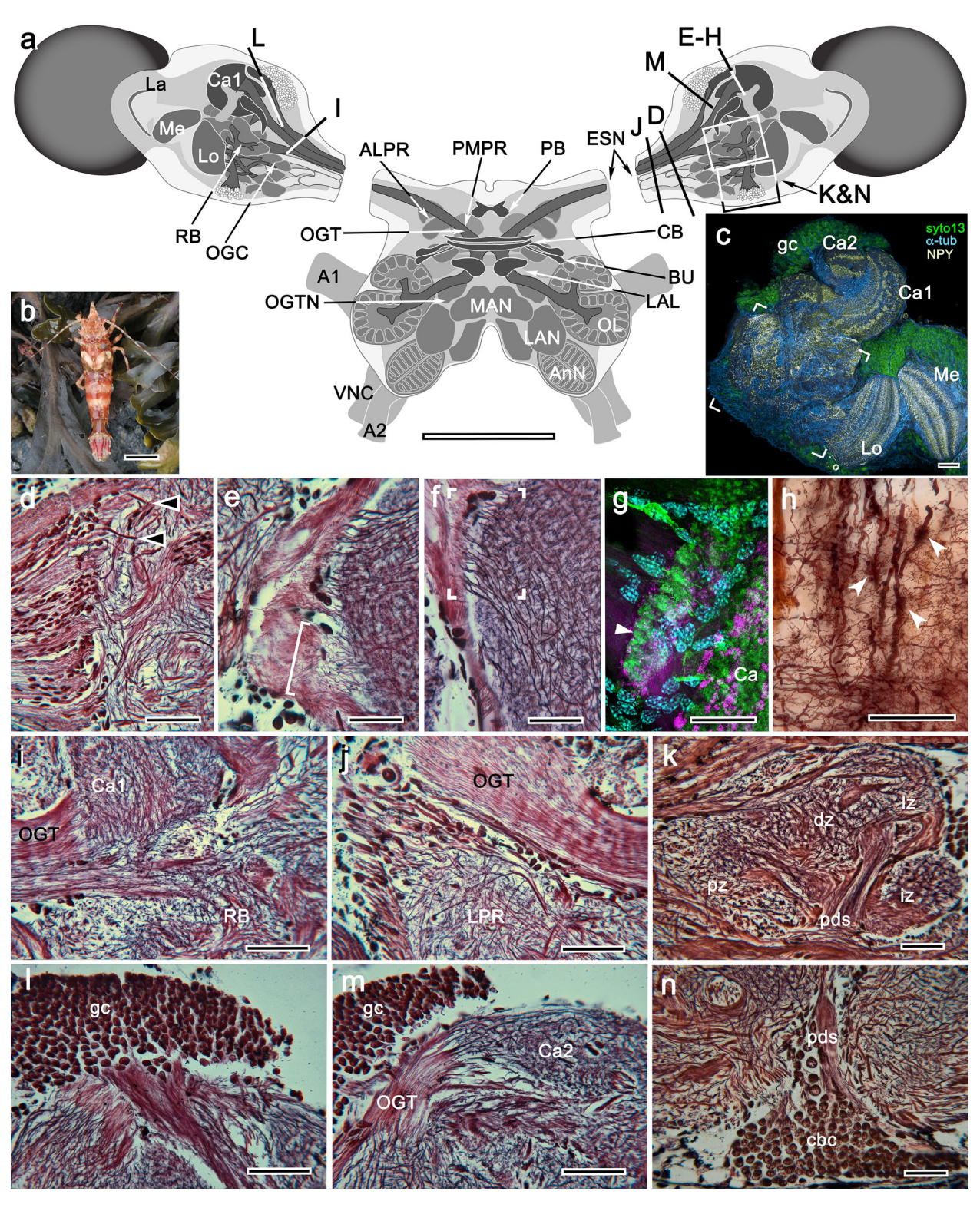


FIGURE 1 Legend on next page.

.0969861, 2019, 14, Downloaded from https://onlinelibrary.wiley.com/doi/10.1002/cne.24678 by University Of Arizona Library, Wiley Online Library on [22/02/2024]. See the Terms

and Conditions (https://onlinelibrary.wiley.com/term

ditions) on Wiley Online Library for rules of use; OA articles are governed by the applicable Creative Commons

reverse ( $\alpha$ -terpineol was omitted during the rehydration). Following the rehydration series, slides were placed in a coplin jar containing double distilled (dd) H<sub>2</sub>O. Next, the slides were transferred to a coplin jar containing 2.5 g silver proteinate (Protargol; Winthrop Chemical Co., NY) and 5 g copper shot and left to incubate at 60°C overnight. Prior to incubation, the fine copper shot pellets were cleaned by rinsing in 3% nitric acid diluted with ddH2O for 5 min.

The following day, the coplin jar containing the slides was removed from the oven and allowed to cool to RT. The sections were then rinsed in ddH2O for 15 s and transferred into a developer containing 1% hydroquinone and 2% sodium sulfite (Sigma Aldrich; Cat# H9003; Cat# S0505, respectively; St. Louis, MO) in ddH2O for 5 min. Next, the tissue sections were briefly rinsed in tap water for a duration of 3 min and then quickly rinsed twice in ddH2O water. Sections were then submerged in a solution containing 1% filtered gold chloride (Fisher Scientific; Cat# G54) in ddH2O under strong light for 10 min. Following gold toning, the slides were rinsed in two changes of ddH2O at 30 s intervals before being transferred into a solution of 2% oxalic acid (Sigma Aldrich; Cat# 75688; St. Louis, MO) for 8 min. Next, the slides were rinsed in two changes of ddH2O, 1 min each, and left to incubate in 5% sodium thiosulfate for 5 min. Last, slides were rinsed in ddH2O and then dehydrated through an ethanol series of 50, 70, 90, 100% and into 100% xylenes at 5-min intervals and mounted under glass coverslips using Entellan mounting medium (Sigma Aldrich; Cat# 1.0796; St. Louis, MO).

## 2.4 | Antibodies

A variety of antibodies were used in this study to aid the visualization of neuronal processes and their organization in defined neuropils (Figures 1c,g; 3a,b; 4 f-k; and 5 a-g). Antibodies and their provenance are provided in Table 1. The number of *Lebbeus* treated with each antibody is provided in this table; "n" represents the number of animals with

each animal contributing a single pair of eyestalks. Antibodies against synapsin and α-tubulin were used to identify synaptic densities and cytoskeletal elements, respectively. These antibodies have been used in previous studies to identify synaptic and structural connectivity across distant groups of invertebrate phyla, suggesting that they both recognize highly conserved epitope sites (Andrew, Brown, & Strausfeld, 2012; Brauchle, Kiontke, MacMenamin, Fitch, & Piano, 2009; Harzsch, Anger, & Dawirs, 1997; Harzsch & Hansson, 2008; Klagges et al., 1996; Sullivan, Benton, Sandeman, & Beltz, 2007; Thazhath, Liu, & Gaertig, 2002). Tyrosine hydroxylase (TH), the enzyme converting tyrosine to dopamine, and glutamic acid decarboxylase 65/67 (GAD), which catalyzes decarboxylation of glutamate to GABA, were both used as primary antibodies because they do not require fixation with glutaraldehyde. Previous colabeling studies have revealed that both antibodies reliably label either dopaminergic neurons or GABAergic neurons when used in conjunction with their aminergic derivatives, and are thus a suitable replacement for those antibodies which require alternative fixation methods (Cournil, Helluy, & Beltz, 1994; Crisp, Klukas, Gilchrist, Nartey, & Mesce, 2001; Stemme, Iliffe, & Bicker, 2016; Stern, 2009). A polyclonal antibody, DCO, which was developed to detect the catalytic subunit of protein kinase A (PKA) in Drosophila melanogaster and which has been shown to be required for learning and memory (Crittenden, Skoulakis, Han, Kalderon, & Davis, 1998; Skoulakis et al., 1993), was used in this study to detect regions that may be likewise involved in Lebbeus. Western blots, comparing tissue from malacostracan crustaceans and insects, as well as remipedes and insects, have shown that this particular antibody recognizes the expected band across orders (≈40 kD; Stemme et al., 2016; Wolff, Harzsch, Hansson, Brown, & Strausfeld, 2012). Visualization of neuronal processes was further aided by the use of a polyclonal antibody against serotonin (5HT). Serotonin is a neurotransmitter that is ubiquitous across Arthropoda and has been previously used to characterize neuronal architecture across species (Antonsen & Paul, 2001; Harzsch &

FIGURE 1 Overview of Lebbeus groenlandicus whole brain with lateral protocerebrum neuroarchitecture. (a) Schematic of L. groenlandicus brain and major neuropils. Levels labeled D-N in schematic correspond to panels labeled d-n below. Abbreviations: A1, antennular nerve 1; A2, antennal nerve 2; ALPR, anterior lateral protocerebral lobe; AnN, antenna 2 neuropil; BU, lateral bulb of the central complex; Ca1, Ca2, Calyx 1, 2; CB, central body; ESN, eyestalk nerve; La, lamina; LAL, lateral accessory lobe of the central complex; LAN, lateral antennular neuropil; Lo, lobula; MAN, median antenna 1 neuropil; Me, medulla; OL, olfactory lobe; OGC, optic glomeruli cluster; OGT, olfactory globular tract; OGTN, neuropil of the olfactory globular tract; PMPR, posterior median protocerebral lobes; PB, protocerebral bridge; RB, reniform body; VNC, ventral nerve cord connective linking the supraesophageal brain to gnathal ganglia and ventral ganglia. (b) Top-down view of an adult Lebbeus shrimp. (c) Confocal laser scan of sectioned eyestalk tissue colabeled with antibodies against neuropeptide Y (NPY; beige), \( \alpha \)-tubulin (cyan) and the nuclear stain syto13 (globuli cell bodies [gc]; green). The boxed area includes numerous circumscribed neuropils that contribute to the lateral protocerebrum in addition to the calyces and optic lobe neuropils. (d-f, i-n) Bodian stained sections of Lebbeus mushroom body and lateral protocerebral neuropil. (f) Afferent axons projecting to the most basal region of the eyestalk. Axons from the olfactory globuli tract (OGT) diverge here and project to regions within the lateral protocerebrum and mushroom body calyx. Some axons with particularly large diameters (arrowheads) derive from the lateral antennular lobe neuropils (LAL). (e) Axons enter the calyces from two distinct fascicles from the OGT, one of which is populated by extremely-small-diameter axons that reach layer 3 of the calyx (bracketed). (f) Parallel arrangement of OGT afferents in the calyx. The boxed area is equivalent to panel (g), showing a confocal laser scan of a row (arrowhead) of glia-like cells bordering the calyx, as revealed by anti f-actin (green) and the nuclear label syto13 (cyan). Microglomeruli in the calyx neuropil (Ca) are denoted by the punctate labeling of anti-synapsin (magenta). (h) Golgi impregnation of afferent axons arborizing in the calyx with dense, brush-like terminals (arrowheads). (i) Axon bundles from the OGT bifurcate, sending projections to the mushroom body calyx (Ca1) and the reniform body (RB). (j) Small diameter axons of the OGT projecting past neuropils of the dorsal region of the lateral protocerebrum (LPR), which is supplied by larger diameter axons. (k) The reniform body (RB in panel a). Situated just ventral-lateral to the mushroom body, the reniform body is formed by processes, originating from a cell body cluster (cbc; panel n), that provide synaptic neuropils to four major zones: the dorsal (dz), initial (iz), lateral (lz), and proximal zones (pz). (I) Dense population of globuli cells (gc), which in both calyces gives rise to dendritic process, from which projections extend into the mushroom body columns (see, Figure 3). (m) OGT fibers projecting into the smaller of the two calycal regions (Ca2; see Figure 2). (n) Cell body cluster (cbc) with axonal tributaries projecting via the cell body fiber pedestal (pds) into the reniform body. Scale bars = a, 1 mm; b, 1 cm; c, 100 µm; d-f 50 µm; g, 25 µm; h-n, 50 μm [Color figure can be viewed at wileyonlinelibrary.com]

of use; OA articles are governed by the applicable Creative Commons

**TABLE 1** Antibodies used and their source; number of applications (n = number of animals used; each animal contributes a single pair of eyestalk neuropils)

Antibody	Immunogen	Host	Concentration	Supplier; catalogue #; RRID	Number of applications (n = 28 total)
α-Tubulin	$\alpha\text{-}Tubulin$ derived from the pellicles of the protozoan $\textit{Tetrahymena}$	Mouse (monoclonal)	1:100	DHSB; 12G10; AB_1157911	n = 18
α-Tubulin	Synthetic peptide within human alpha tubulin; amino acid 400 to the c-terminus	Rabbit (polyclonal)	1:250	Abcam; ab15246; AB_301787	n = 6
Synapsin (SYNORF1)	Drosophila melanogaster glutathione S-transferase-fusion protein	Mouse (monoclonal)	1:100	DSHB; 3C11; AB_528479	n = 4
DC0	Alpha catalytic subunit of protein kinase A	Rabbit (polyclonal)	1:400	Generous gift from Dr. Daniel Kalderon	n = 6
GAD	C-terminal of both the 65- and 67-kDa isoforms of human GAD	Rabbit (polyclonal)	1:500	Sigma Aldrich; G5163; AB_477019	n = 6
Serotonin (5HT)	Serotonin coupled to bovine serum albumin with paraformaldehyde	Rabbit (polyclonal)	1:1,000	ImmunoStar; 20,080; AB_572263	n = 4
TH	TH purified from rat PC12 cells	Mouse (monoclonal)	1:250	ImmunoStar; 22,941; AB_572268	n = 6
NPY	Residues 1 to the C-terminus of pig NPY	Rabbit (polyclonal)	1:250	Abcam; ab30914; AB_1566510	n = 2

Abbreviations: GAD: glutamic acid decarboxylase; NPY: neuropeptide Y; TH: tyrosine hydroxylase.

Note: Most of the antibodies used in this study were used in combination; hence the total sum of applications listed per antibody in this table will be greater than 28.

Hansson, 2008; Nässel, 1988), including in neurophylogenetic analyses (Harzsch, 2004; Harzsch & Waloszeck, 2000). Last, an antibody against vertebrate neuropeptide Y (NPY) was used to further delineate neuropil boundaries. Vertebrate NPY is likely to be ancestrally related to insect neuropeptide F, both of which have been implicated in feeding, stress response, metabolism, and reproduction in vertebrates and invertebrates, respectively (Nässel & Wegener, 2011). Antibodies against NPY, TH, GAD, and 5HT were quality control tested by the manufacturer using standard Immunohistochemical methods.

#### 2.5 | Immunohistochemistry

Shrimps were cooled to immobility over ice, and nervous tissue was dissected out in cold fixative containing 4% PFA (Electron Microscopy Sciences; Cat# 15710; Hatfield, PA) and 10% sucrose in 0.1M phosphate buffered saline (PBS; Sigma Aldrich; Cat# P4417; St. Louis, MO). Tissue was left in fixative solution overnight at 4°C. Brains were rinsed twice in PBS the following day. Following the rinse cycle, tissue was embedded in a mixture consisting of 5% agarose and 7% gelatin (as described by Long, 2018) and sectioned at 60 μm using a vibratome (Leica; Nussloch, Germany). Subsequent sections were then rinsed twice in PBS containing 0.5% Triton-X (PBST; Electron Microscopy Sciences; Cat# 22140; Hatfield, PA) over the course of 20 min and blocked in 0.5% PBST containing 5% normal donkey serum (Jackson Immuno-Research; RRID:AB\_2337258; West Grove, PA) for 1 hr. Primary antibody was then added to the solution and left overnight at RT on a gentle shake. No demasking step was required for GAD immunolabeling in L. groenlandicus, as has been reported in previous studies (Langeloh, Wasser, Richter, Bicker, & Stern, 2018; Stemme et al., 2016).

The next day, sections were rinsed with 0.5% PBST for 1 hr. Meanwhile, 2.5 µL of IgG secondary antibodies raised in donkey and conjugated to either Cy3, Cy5, or Alexa 647 fluorophores (Jackson ImmunoResearch; RRID:AB\_2340813; RRID:AB\_2340607; RRID: AB\_2492288, respectively; West Grove, PA) were added to 1,000 μL of 0.5% PBST and centrifuged at 11,000g for 15 min. The top 900  $\mu L$  of the secondary antibody solution was taken and added to the sections, which were then left on a gentle shake overnight in the dark at RT. The following morning sections were rinsed twice in 0.5M Tris-HCl buffer (pH 7.4; Sigma Aldrich; Cat# T1503; St. Louis, MO). To stain cell nuclei, tissue was then incubated in either Syto-13 or Syto-16 (ThermoFisher Scientific; Cat# S7575, Cat# S7578 respectively: Waltham, MA) at a concentration of, 1:2,000 for 1 hr. Next, sections were rinsed in Tris-HCl buffer six times over the course of an hour and then mounted on glass slides using a mounting medium containing 25% polyvinyl alcohol, 25% glycerol, 50% PBS and covered using #1.5 coverslips (Fisher Scientific; Cat# 12-544E; Hampton, NH). Control experiments in which the primary antibody was omitted resulted in complete elimination of staining.

For F-actin staining, sections were left to incubate in 0.5% PBST containing 1:40 phalloidin conjugated to Alexa 488 (ThermoFisher Scientific; RRID:AB\_2315147; Waltham, MA) following secondary antibody incubation for 2–3 days. The sections were agitated on a shaker and left at RT in the dark for the duration of incubation.

TH immunolabeling required a specialized protocol which included a shorter fixation time and antibody labeling of whole mount tissue prior to sectioning. Fixation times lasting longer than 1 hr resulted in reduced or no immunoreactivity [this was also reported in Lange and Chan (2008)].

Similarly, immunoreactivity was best preserved when the tissue was labeled as a whole mount prior to sectioning (also reported in Cournil et al., 1994).

For TH immunolabeling, neural tissue was fixed at RT for 30–45 min and then rinsed twice in PBS. Whole brains and eyestalks were then rinsed twice in 0.5% PBST and left to block in 1% PBST containing 5% normal donkey serum for 3 hr. Next, TH primary antibody was added to the solution at a concentration of 1:250 and the tissue was subjected to microwave treatment. The microwave was temperature controlled at 18°C, and the tissue was exposed to two cycles of 2 min under low power and 2 min under a vacuum. Whole mount tissue was left for 2–3 days at RT on a shaker and was subjected to microwave treatment each day. After primary antibody incubation, the tissue was rinsed in 0.5% PBST over the course of 3 hr and treated with Cy3-conjugated IgG antibodies as described for the sectioned material. Following secondary incubation, the brains were embedded, sectioned, and processed also as described above.

#### 2.6 | Imaging

Confocal images were collected using either a Zeiss Pascal 5 or LSM880 confocal microscope (Zeiss; Oberkochen, Germany). Image projections were made using FIJI (z project plugin; Schindelin et al., 2012). Brightness, contrast, and color intensity were adjusted using Adobe Photoshop CC (Adobe Systems Incorporated; San Jose, CA). Light microscopy images were obtained using a Leitz Orthoplan microscope. Series of step focused image sections (0.5–1 µm increments) were stitched together and then reconstructed using Helicon Focus (Helicon Soft; Kharkov, Ukraine).

#### 2.7 | Terminology

Correspondences between the mid-protocerebrum of insects and crustaceans are hallmarked by the central body and its satellite neuropils, such as the lateral bulbs and lateral accessory lobes (Figure 1a) that together constitute the central complex (Thoen, Marshall, Wolff, & Strausfeld, 2017). In light of similarities of the insect and crustacean protocerebrum, we employ, where possible, terminology established for insect brains (Ito et al., 2014). Names referring to neuronal features in the deuto- and tritocerebrum peculiar to crustaceans follow, or are adapted from, recent published descriptions (e.g., Tuchina et al., 2015).

## 3 | RESULTS

# 3.1 | Lebbeus brain organization is typical of Eumalacostraca

Hexapods originated from within paraphyletic Crustacea (Oakley, Wolfe, Lindgren, & Zaharoff, 2013; Regier, Shultz, & Kambic, 2005; Schwentner et al., 2018; von Reumont et al., 2012). While crustacean and insect brains share some obvious correspondences, there are crustacean neuropils that may have no insect counterpart. Also, many lineages have been subject to the evolved reduction or loss of specific neuropils, as in Maxillipoda and Xenocarida (Remipedia + Cephalocarida) or in eumalacostracan genera that have adopted life in

the water column (Andrew et al., 2012), complete darkness (Stegner, Stemme, Iliffe, Richter, & Wirkner, 2015) or terrestrialization (Harzsch et al., 2011). Nevertheless, as in insects, the ground pattern of the crustacean brain is the fusion of the central nervous system's three most anterior segmental ganglia: the protocerebrum contiguous with the deuto- and tritocerebra, all sharing numerous integrative pathways. The first two ganglia lie above the stomodeum with the tritocerebrum partially dorsal to and also flanking the gut. Axons leaving and entering the brain comprise the paired ventral cords, connecting all subsequent ganglia beneath the gut.

The disposition of major integration centers that serve as landmarks in the brain, by and large, correspond in the malacostracan, remipede, and insect protocerebrum. However, there are some important differences relating to the deuto- and tritocerebra. Two that are relevant to Lebbeus refer to the olfactory lobes, long considered homologous across Pancrustacea. In Lebbeus (Figure 1a), as in other malacostracans, the olfactory lobes are supplied by axons from olfactory receptor neurons on the lateral flagellum of the antennules, which in malacostracans are branched. The representation of olfactory receptor neurons in the olfactory lobes differs anatomically from that in the insect olfactory lobes (traditionally referred to as "antennal lobes"). These distinctions are further elaborated in the Section 4. In malacostracans, somatotopically organized bimodal chemo- and tactile receptor neurons on the antennules supply a second prominent neuropil called the LAN (Figure 1a), for which there is no obvious counterpart in insects. Also, unlike insects, crustaceans possess a pair of appendages at the level of the tritocerebrum. These are the antennae, which also provide tactile and chemosensory inputs to a somatotopically organized "antennal neuropil" (AnN, Figure 1a).

As in many crustaceans, in *Lebbeus* the protocerebrum extends forwards from its sides such that many of its lateral neuropils, including those cardinal to multisensory integration, reside within the swollen terminal article of its eyestalks (Figures 1a,c and 4a,b). These lateral protocerebral neuropils comprise the nested optic lobes and, central to them, numerous discrete synaptic neuropils (Figures 1c and 4a). These include the optic glomeruli that receive segregated outputs from the lobula (Figure 1a), as they do in insects (Mu, Ito, Bacon, & Strausfeld, 2012). In the literature, the assemblage of neuropils proximal to the optic lobes are commonly referred to as a single entity called the "medulla terminalis" (Sandeman, Kenning, & Harzsch, 2014). However, there are two accounts that distinguish some of its discrete neuropils (Blaustein, Derby, Simmons, & Beall, 1988; Sullivan & Beltz, 2005).

Studies of malacostracan brain evolution have generally focused on the organization of the central brain dissociated from lateral neuropils linked to it by the eyestalks (Sandeman et al., 2014). However, those neuropils are crucial in phylogenetic interpretations because they participate in the brain's most crucial functions: multimodal sensory integration, learning and the establishment of memories (Mellon, 2000; Sullivan & Beltz, 2004). The eumalacostracan lateral protocerebrum contains not only the optic lobes and their central targets but the prominent multisensory integration center hitherto known as the hemiellipsoid body that receives its major input from the olfactory lobes, as well as from haptic and chemosensory pathways (Sullivan & Beltz, 2004). Also included in the lateral

FIGURE 2 Afferent nerve fiber terminals in the Ca1 calyx of the *Lebbeus* mushroom body. (a) Golgi impregnated sections reveal the morphology of putative presynaptic ensembles of olfactory globular tract (OGT) afferent endings into ensembles of dendritic trees corresponding to crayfish parasol cells (McKinzie et al., 2005). These are intersected by small (arrowed white), medium (arrowed black), and large diameter efferents (black arrowheads). Large afferents are decorated by tufted presynaptic zones (white arrowheads). Three distinct regions in the calyx are denoted by the brackets 1–3, layer 1 being most distal and is further divided into three strata (for layering, see also Figures 3–5). (b) Layer 1 is further subdivided into three strata, the outermost denoted by bundles of incoming afferents from the OGT (large black arrows). The second and third strata are denoted by tangentially extending local interneuron processes, the densest indicated by a white arrowhead. Numerous small to medium climbing afferents extend centrifugally into layer 1 (small white and black arrows) from deeper levels. (c, d) Axons projecting into the main calycal region of the mushroom body (Ca1) end as extended terminals that vary in morphology from those decorated by small bead-like specializations (black arrows) or varicosities (black arrows). Larger terminals are decorated by dense, brush-like morphologies (white arrowheads). (d) Cross sections of afferent bundles in the outermost layer (black arrows; also, in (b) arranged orthogonal to the afferent projections in strata 2 and 3. Scale bars = a–d, 50 μm

protocerebrum is the reniform body, an elaborate arrangement of 3–4 neuropils that appears to have no counterpart in Hexapoda (Figure 1a,k,n), and which may correspond to a center identified by Sullivan and Beltz (2005) in the crayfish *Cherax destructor*, termed the diamedullary neuropil (cit. Loc. Figure 5f).

#### 3.2 | The Lebbeus mushroom bodies: an overview

The "hemiellipsoid body" of L. groenlandicus consists of two adjacent neuropils both stratified into distinct layers and both supplied by neurons originating from globuli cells arranged as a dense cluster above them (Figure 1c). The hemiellipsoid body is hereon referred to as the mushroom body calyx by virtue of an organization that corresponds in detail to that of the insect calyx and the more elaborate calyx of the stomatopod mushroom body (Wolff et al., 2017). As in insects, where Kenyon cells are the intrinsic neurons of the mushroom bodies, intrinsic neurons in Lebbeus comprise identical components. Each intrinsic neuron consists of a minute basophilic cell body (traditionally referred to as a "globuli cell") from which extends a slender neurite. This thickens and then gives rise to a system of dendritic branches. A slender axon-like extension contributes to the columnar lobe arising from the inner face of the calyx. Many thousands of globuli cells form a dense cluster above the lateral protocerebrum's rostral surface and, consequently, many thousands of intrinsic neuron dendrites form the

bulk of the calyx, which receives inputs from the sensory relay neuron axons carried by the olfactory globular tract (OGT) as well as relays from other sensory neuropils (Figure 2). The axon-like extensions of the intrinsic cell neurites form the bulk of the columnar neuropil that extends from the calyces (Figure 3). This corresponds to the columnar lobe of an insect mushroom body, and as in insects the columns in Lebbeus are strongly immunoreactive to antibodies raised against DCO, the major catalytic subunit of Drosophila c-AMP-dependent PKA (Lane & Kalderon, 1993). This antibody identifies the mushroom body columns of all surveyed insect genera other than Archaeognatha (Farris, 2005), as well as corresponding centers in Myriapoda, Arachnida, and polychaete annelids (Wolff & Strausfeld, 2015a). In Lebbeus, the mushroom body columns consist of intrinsic neuron processes intersected at discrete domains by efferent and afferent trees, certain of which are resolved using antisera raised against GAD, the precursor of the inhibitory transmitter γ-aminobutyric acid, serotonin, and TH. These orthogonal network arrangements, their immunological identities (Figures 3a,b and 4f-k) and fiber architectures (Figures 3f-i and 4e) correspond to the insect mushroom body ground pattern where sequential synaptic domains of the mushroom body's columnar lobes relate to functionally segregated outputs having characteristic immunohistological identities and integrative functions (Aso et al., 2014; Hamanaka, Minoura, Nishino, Miura, & Mizunami, 2016; Nässel & Elekes, 1992).

FIGURE 3 DC0 immunoreactivity and neural composition of the mushroom body calyces and columns. (a, b) Confocal laser scans showing elevated expression of DC0 (magenta) in columns 1 (Clm1), 2 (Clm2), the dorsal zone of the reniform body, and calycal levels 1-3. Sections are also labeled with  $\alpha$ -tubulin (cyan) and syto13 (green). Cross sections of bundled afferent axons are resolved by α-tubulin in the outer level of Ca1 (arrows). Syto13 resolves the dense arrangement of globuli cells (gc), some strongly labeled with DC0, clustered above the calyces and lobes. Column 1 is a sausage-shaped lobe. Column 2 terminates as several tubercle-like domains (asterisks). The inset lower left in panel (a) shows microglomeruli in Clm1, revealed by synapsin-actin immunolabeling (synapsin, pink; Factin, green; syto13, cyan). (c-i) Light microscopy images of Golgi-impregnated neuropils of the calyces and lobes. (c) Surface view showing the serried arrangement of intrinsic neuron processes entering the outer level of Ca1. The inset upper right shows a top-down view of a single clawed Kenyon cell dendritic tree. (d) The outer level of Ca1 showing dendritic trees of spiny intrinsic neurons. Climbing afferent terminals, from lateral protocerebral tracts (white arrows) extend obliquely among intrinsic cells. The most superficial stratum of the Ca1 also contains tangentially directed processes (black arrow) of local interneurons within the calyx. (e) Layering in the calyx: Layer 1 comprises intrinsic neuron dendritic trees that correspond to parasol cells identified in crayfish (McKinzie et al., 2005); layer 3 appears denser due to converging intrinsic neuron processes and extension into the root of the Clm1 column (asterisk). (f) Processes of intrinsic neurons in Clm1 that are decorated with beaded swellings and spines indicative of presynaptic and postsynaptic sites. (g) The dense dendritic domain of an efferent neuron extending across intrinsic neuron processes in Clm1. (h) The trajectory of intrinsic neuron processes comprising Clm2 providing tubercle-like domains of terminals (asterisks), also asterisked in panel (b). (i) Dendritic arborization of an output neuron from a Clm2 tubercle. Scale bars = a, b, 100 μm (inset to a, 50 μm); c-e, h, i, 50 μm (inset to c, 20 μm); f, g, 25 μm. Bracketed area in panel (a) is same area as framed in panel (e), bracketed area in panel (b) corresponds to format of panel (h)

FIGURE 4 Organization of mushroom body columns. (a) Schematic representation of the *Lebbeus* right lateral protocerebrum, optic lobe (lamina, La; medulla, Me; lobula, Lo), mushroom body (MB) and reniform body (RB). Other neuropils indicated in gray tones. (b) Enlargement of MB showing its calycal (Ca1, 2) neuropils, columns (Clm1, Clm2), and globuli cells (gc, green). (d, e) Bodian-stained sections of the MB. (c) The dense arrangement of globuli cells provide massed cell body fibers (neurites, neu) to the three calycal levels in Ca1 (bracketed 1–3); Ca1 also receives terminals supplied by axonal bundles (white arrows) from the lobula, optic glomeruli, and RB. Other tracts (black arrows) carry information to and from the Clm1 column. (d) Mushroom body intrinsic neuron processes in Clm2 terminate as tubercle-like synaptic domains (asterisks) that are richly innervated by aminergic inputs (panels j, k). (e) The Clm1 column (corresponding to area delineated by corner brackets in panel (c) showing intrinsic neuron processes in their characteristic orthogonal arrangement. (f) Elevated levels of DC0 expression (magenta) provide contrast to the α-tubulin-immunoreactive afferent and efferent processes (cyan) extending across the Clm1 column. (g) DC0-positive tubercular domains in Clm2. Asterisks show matching arrangements with those indicated in panel (d). (h) Tyrosine hydroxylase (TH) immunoreactivity in Clm1 reveals very fine processes at discrete regions along the column. (i, j) Glutamic acid decarboxylase immunofluorescence (yellow) in Clm1 (i) and Clm2 (j). (k) Innervation of Clm2 domains by TH-immunoreactive processes. Scale bars = c, d, 100 μm; e-g, 50 μm; h, 10 μm; i-k, 25 μm

# 3.3 | Organization of the mushroom body calyces and their afferent supply

Situated dorsally in the eyestalk neuropil (Figure 1a), the *L. groenlandicus* mushroom body can be recognized by its massive size dominating underlying neuropils and the optic lobes (Figures 1c, 3a,b, and 4a–d). The mushroom body calyces receive their chemosensory supply from multiglomerular projection neurons in the antennular (olfactory) lobes, the axons of which initially ascend into the midbrain via the left and right OGT (Figure 1a) to converge at the protocerebrum's midline just ventral to the central

body. Numerous axons bifurcate sending one tributary ipsilaterally and one contralaterally into the eyestalk nerves (ESN, Figure 1a). Axons from the LAN (Figure 1a) join the OGT near the level of the OGT neuropil (Figure 1a). In the eyestalk nerve, the OGT lies dorsally with respect to larger diameter axons. These belong to relay neurons extending from the medial protocerebrum outwards to the lateral protocerebrum and to neurons that extend in the other direction from the lateral protocerebrum to the medial protocerebrum, some crossing the brain to reach the contralateral lateral protocerebrum.

FIGURE 5 Immunoreactivity in the *Lebbeus* mushroom body calyx. Confocal laser scans of immunohistochemically stained sections. (a) Concentric layering (bracketed 1–3) in the calyx is revealed by synapsin labeling (magenta) in Ca1 of the mushroom body. (b) Distribution of glutamic acid decarboxylase (GAD, yellow) in both calyces (Ca1 and Ca2). Also shown are abundant intrinsic cell neurites (neu, cyan; α-tubulin labeling) extending into the calyx from globuli cell cluster (gc). GAD-immunoreactive fibers supply most of the calyx with the notable exception of layer 2 (denoted by brackets). (c) 5HT labeling (pink) of feedback neurons innervating both calyces as well as dense labeling in the reniform body. (d) Large tyrosine hydroxylase (TH)-immunoreactive feedback neuron to both calyces, the processes of which are concentrated in the outer (first) layer. (e) Delicate serotonergic afferents (yellow) with abundant ramifications through the second stratum (bracketed) of the outer level of Ca1. Serotonergic afferents also reach out to neuron bundles entering the outer stratum, revealed by α-tubulin labeling (arrows). (f) TH immunoreactivity in the second stratum of the calyx's outer level (bracketed). (g) Neuropeptide Y (NPY)-labeled section of Ca1 depicting large NPY-positive clusters of profiles alongside and beneath bundled axonal processes (arrow). Scale bars = a-d, 100 μm; e-g, 25 μm

Axons of olfactory lobe projection neurons are extremely slender in the OGT within the eyestalk nerve, measuring less than 1.5  $\mu m$  in diameter. But subsets of these can expand to up to 2-3 µm in diameter just before penetrating superficial layers of the major (Ca1) and minor (Ca2) calyces (Figure 1d-f). These various sizes of afferent fibers can be resolved by reduced silver and Golgi impregnation (Figures 1d-f,h and 2a,c,d). At least 20,000 axons are estimated to reach the lateral protocerebrum from the OGT. A single layer of glial cells is arrayed along the border of the calyces, where OGT nerve bundles appear to delaminate and sort into parallel fibers as they enter and then extend across the calyx (Figure 1g). Golgi impregnations show terminals from the OGT decorated with bead-like, varicose, or bottle brush-like presynaptic areas (Figures 1h and 2a,c,d). As such, they correspond to the morphologies of afferent endings in the insect mushroom body calyx (Strausfeld & Li, 1999). In Lebbeus, after entering the lateral protocerebrum, the OGT branches, providing its major inputs to the calyces and smaller tributaries to several discrete neuropils beneath the mushroom bodies. This is comparable to olfactory pathways in insects, which already have distinct exit points from the olfactory lobes and which adopt distinctive trajectories to the calyces as well as other neuropils in the lateral protocerebrum (Galizia & Rössler, 2010). Comparable arrangements where bundles of axons from the OGT diverge, with some supplying the calyx and others to neuropils beneath it, have been described from the pink shrimp *Penaeus duorarum* and the mantis shrimp *Gonodactylus bredini* (Sullivan & Beltz, 2004).

As demonstrated by immunohistology and Bodian silver staining (Figures 3a,b, 4c,d, and 5a,b) the calyces are organized into three concentric layers, the outermost of which is further stratified by arrangements of afferent endings and processes of GAD-, 5HT-, and TH-immunoreactive feedback neurons (Figure 5). Terminals from the OGT enter various levels of the outer calycal layer where they intersect the dendritic branches of its intrinsic neurons (Figure 2a). These are supplied by 3,000–4,000 globuli cell bodies that are densely clustered rostrally in the lateral protocerebrum, immediately above the entrance of the OGT (Figures 1a, 3a,b, and 4c,d). Cell body fibers (neurites) extend unbranched until the intermediate (mainly immunonegative) layer 2 of the calyx (Figure 3e). There, the neurites branch to

provide distal dendrites from an axon-like process that extends perpendicularly through subsequent levels of the calyx (Figures 2a and 3e). Two dendritic morphologies have been identified: those with claw-like synaptic specializations (inset to Figure 3c) and others with spiny dendrites (Figure 3d). These morphologies are comparable to clawed and spiny Kenyon cell dendrites of the insect calyx (Wolff et al., 2017). Together, intrinsic neurons form a dense palisade across the calyx, each neuron contributing a broad dendritic tree to the crammed outer canopy that comprises calyx layer 1 (Figures 2a and 3d,e). This outer layer is strongly immunoreactive to antibodies raised against synaptic proteins, DCO, serotonin (5HT), as well as against GAD, TH, and NPY (Figures 1c, 3a,b, and 5). Layer 1 is further subdivided into three narrower strata defined by the layered arrangements of tangentially directed OGT afferents, local interneurons, and afferents originating from lateral neuropils extending centrifugally outwards from the inner face of the calyx (Figure 2b-d). These stratified arrangements are also reflected by the distribution of 5HT, TH, and synapsin (Figure 5). Layer 3, the deepest level of the calyces, comprises axon collaterals from intrinsic neurons as well as interneuron processes and terminals supplied by axon bundles originating in the optic lobe's lobula, optic glomeruli, and reniform body (Figure 4c). These origins confirm the multimodal nature of the calyx. Calycal layer 3 is also heavily invested with GAD-labeled profiles (Figure 5b) but has relatively sparse arrangements of profiles labeled with anti-5HT, at least in Ca1 (Figure 5c). In the smaller calyx (Ca2), 5HT labeling clearly identifies the outer and inner layers of this neuropil. TH labeling is mainly confined to layer 1 in both calyces (Figure 5d,f).

## 3.4 | Origin and organization of the mushroom body columns

In insects, Kenyon cells, which are the mushroom body's intrinsic neurons, extend long parallel processes that comprise the bulk of the mushroom body's columnar lobes. In L. groenlandicus intrinsic neurons provide a corresponding arrangement. There are two lobes in L. groenlandicus, each denoted by their elevated affinity for antibodies raised against DCO (Figures 3a,b and 4f,g). And, as in some insect species, even in the calyx (Ca1) intrinsic neurons can be labeled with this antibody (Figure 3a). DC0 identifies two columns (Clm1, Clm2), the larger of which (column 1; Figure 3a) originates from the larger of the two calyces (Ca1). Bodian reduced-silver sections reveal this lobe's characteristically interwoven processes, which impose an orthogonal network throughout the column's length (Figure 4e). These are also resolved by Golgi impregnations (Figure 3f). The processes are decorated with bead-like swellings and spines indicative, respectively, of presynaptic and postsynaptic sites (Strausfeld & Meinertzhagen, 1998). Dense arrangements of afferent and efferent trees that occupy discrete domains along the length of the column intersect the intrinsic cell processes (Figures 3g and 4f). This organization is distinct from that of the second column Clm2, the processes of which are mainly recruited from both the large and small calyces (Ca2). Initially the processes of Clm2 project in parallel, tightly bundled and devoid of synaptic specializations (Figure 3b). Clm2 processes project toward the proximal margin of the lateral protocerebrum where they give rise to tuberculate islets (Figures 3b and 4d), each of which labels strongly with DC0 (Figure 4g).

Both mushroom body columns (Clm1 and Clm2) are invaded by efferent and afferent arborizations revealed in Golgi impregnations as richly decorated with synaptic specializations (Figure 3g,i). Immunoreactivity to TH and to GAD also resolves efferent and afferent neurons intersecting the passage of intrinsic neuron processes. TH-immunoreactive processes in Clm1 are distributed as a fine network throughout its neuropil, as are GAD-reactive processes (Figure 4h,i). GAD- and TH-reactive processes in Clm2 are constrained to its discrete tubercles, with a system of TH-positive axons providing recurrent process back toward the calyces (Figure 4j,k). Both Clm1 and Clm2 are associated with numerous fiber tracts carrying afferents to and efferents from them. Some of these can be matched to immunostained elements, such as that indicated by an arrow in Figure 4i, which corresponds to one of three associated tracts indicated in Figure 4c. Others are revealed by  $\alpha$ -tubulin-immunoreactive profiles that stand out against the background of the DCO-labeled matrix (Figure 4f). However, many tracts leading to and from the columns have not yet been traced to other neuropils, with the exception of connections from the lobula and the reniform body to Clm1. The reniform body (Figure 1k,n) has the same lobed arrangement as in the shore crab Hemigrapsus nudus and in the mantis shrimp Neogonodactylus oerstedii (Wolff et al., 2017), and as in those species its lobes also express elevated levels of DCO (RB in Figure 3a). In Lebbeus, as in those two species, the reniform body's intrinsic neurons originate from a cluster of small globuli-like cell bodies disposed ventrally in the lateral protocerebrum close to the margin of the lobula (Figure 1n), as shown in the schematic of Figure 4a (green).

#### 4 | DISCUSSION

## 4.1 | Electrophysiology points to mushroom bodies in crustaceans

That the names "mushroom body" and "corpora pedunculata" have always referred to a stalked neuropil may account for the difficulty of those studying crustacean brains in identifying a suitable crustacean homologue, despite the genealogical relationship of Crustacea and Hexapoda (Regier et al., 2005). Even Collembola and Diplura, two sister groups of Insecta, possess paired structures worthy of the appellation mushroom body (Böhm, Szucsich, & Pass, 2012; Kollmann, Huetteroth, & Schachtner, 2011). However, comparisons of mainly decapod brains have argued against the hemiellipsoid bodies qualifying as a mushroom body homologue, while admitting their possible equivalence due to the location of the hemiellipsoid body in the lateral protocerebrum and its being, in many species, the target of axons that carry olfactory information from the deutocerebrum (Sandeman et al., 2014).

Compelling evidence for a mushroom body-like functional organization of the hemiellipsoid body has, however, been provided by electrophysiological studies of the crayfish lateral protocerebrum, which demonstrated responses by parasol cells to olfactory, visual, and tactile cues (McKinzie, Benton, Beltz, & Mellon, 2003; Mellon, 2000, 2003). Parasol cells are large efferent neurons with dense dendritic trees in the hemiellipsoid bodies, like those shown here in Figure 3d,e, which extend their axons to distant sites in the lateral protocerebrum. The observation that parasol cells derive from globuli cells, the minute



cell bodies clustered above the hemiellipsoid body, was a compelling reason for comparing them with the Kenyon cells of insects, which also derive from minute cell bodies above their mushroom body's calyx. And where one parasol neuron provides a long axon to a target neuropil that is separate from the hemiellipsoid body, many hundreds of such neurons would provide a prominent stalk-like structure (Mellon, Alones, & Lawrence, 1992).

Despite these clear parallels, the discovery of parasol cells did little to change the view, now embedded in the literature, that insect mushroom bodies are hexapod apomorphies whereas hemiellipsoid bodies are apomorphies of crustaceans (Sandeman et al., 2014; Stemme et al., 2016). Yet, mushroom bodies in crustaceans had been identified long ago, in 1882. Except for Hanström's, 1925 paper (Hanström, 1925), and Derby and Schmidt's (2017) survey of crustacean olfaction, very few publications acknowledge Bellonci's beautifully illustrated account (in one of Europe's most ancient and august scientific journals) showing the lateral protocerebrum of Squilla mantis possessing two uninterrupted centers, the corpo emielissoidale and its columnar protrusion, the corpo allungato. For Bellonci there was no question that together these comprise a mushroom body and that they unify the insect and crustacean brain: "Il corpo emielissoidale e il corpo allungato formano cosi un sistema perfettamente paragonabile ai corpi fungiformi o peduncolati che trovansi nel cervello degli insetti" ("The hemiellipsoidal body and the elongated body thus form a system perfectly comparable to the fungiform or pedunculated bodies found in the brain of insects" (Bellonci, 1882).

# 4.2 | Neuroanatomy confirms mushroom bodies in Eumalacostraca

Bellonci's S. mantis belongs to Stomatopoda, which is sister to Eumalacostraca and represents the most stemward branch of that lineage (Schwentner et al., 2018). Recent studies have confirmed that Stomatopoda possesses mushroom bodies and that these share the same 13 neuroanatomical traits that define the mushroom bodies of insects (Wolff et al., 2017), a finding that amplifies the question of whether this is a fascinating example of convergent evolution or an indication that mushroom bodies are ancient structures existing in one form or another in pancrustacean predecessors. The presence of mushroom bodies in other mandibulates (Myriapoda + Diplopoda), in chelicerates, and in Onychophora (Strausfeld, Strausfeld, Stowe, Rowell, & Loesel, 2006; Wolff & Strausfeld, 2015a), would support the latter view (Strausfeld, 2018). However, do other crustaceans belonging to Eumalacostraca possess mushroom body-like centers defined by the same set of traits as those defining those centers in insects? Do the stalked second-order olfactory centers in one of the morphologically simplest crustacean genera, the allotriocarid Cephalocarida (Stegner & Richter, 2011), close to the insect-remipede lineage, reflect an uninterrupted persistence of this center within Eucrustacea? Hutchinsoniella macracantha, the only representative of its clade, also shows the hexapodlike character of possessing homolateral projections from its olfactory lobes to the distal part of its tuberculate lobed neuropil (Stegner & Richter, 2011). Why are columnar protrusions from a calyx, as in Stomatopoda, absent in many crustacean lineages where all that seems to remain is the layered calyx? In species of insects, if a mushroom body lacks one of its components it is invariably the calyx that is absent, not the lobe (Strausfeld et al., 2009). Thus, Allotriocarida (Oakley et al., 2013) embraces two divergent trends: reduced or absent calyces and homolateral OGT projections in Cephalocarida and Hexapoda; and, in Remipedia, the absence of a lobe-like extension from the calyx, which assumes the identity of a hemiellipsoid body receiving heterolateral inputs.

Preliminary observations have demonstrated DC0-positive columnar extensions from the hemiellipsoid bodies of Stenopus hispidus and Alpheus bellulus, two species that are associated with refined spatial memory, as are Stomatopoda (Wolff et al., 2017). Here, we show that L. groenlandicus, a member of the superfamily Alpheoidea, possesses paired mushroom bodies each defined by two adjacent calyces providing two columnar extensions. These mushroom bodies share the same traits as those of stomatopods: prominently stratified calyces, one much larger than another, their intrinsic neurons supplying DC0-positive columns comprising orthogonal networks of processes either along the shaft or in the column's tuberculate domains (Wolff et al., 2017). The shapes and projections of neurons supplied by the globuli cells match descriptions of parasol cells in crayfish, lending support to the interpretation of parasol cells as the equivalent of Kenyon cells (McKinzie et al., 2003). In Lebbeus, the arrangement of efferent and afferent neurons that intercept the intrinsic neuron processes, which extend from the calyces and are positive to antibodies against GAD, 5HT, and TH, further corresponds to the arrangements in stomatopod and insect mushroom bodies.

# 4.3 | Does the radiation of Eumalacostraca support convergence or homology?

With respect to all other eumalacostracan lineages, Stomatopoda is the most ancient. Might one expect, therefore, that if mushroom bodies have undergone divergence in Eumalacostraca, their stomatopod-like morphologies will be represented with least modification in basal lineages, such as the Stenopodidea, whereas lineages that appeared later in geological time would exhibit greater divergence of mushroom body morphology, including reduction and loss?

The assertion based on observations of neuronal arrangements, that crustacean hemiellipsoid bodies are the homologues of insect mushroom bodies comes from studies of the land hermit crab Coenobita clypeatus, an anomuran species belonging to the infraorder Anomala. Individuals of C. clypeatus possess enormous hemiellipsoid bodies, the structure of which may be unique to that infraorder in having many layers of synaptic networks embedded within its matrix (Wolff et al., 2012). In C. clypeatus, these layers express DCO and contain synaptic networks that correspond in detail to synaptic organization in the columnar lobes of the insect mushroom body (Brown & Wolff, 2012). However, it could be argued that because Anomura is a highly derived reptantian lineage, originating approximately 309 million years ago (mya) in the upper Carboniferous (Porter, Pérez-Losada, & Crandall, 2005), the presence of mushroom body-like circuits might have arisen independently by convergent evolution. However, the possibility that a mushroom body circuit has been evolutionarily subsumed into the anomuran hemiellipsoid body and is thus a result of divergent evolution rather than a de

novo convergent acquisition is suggested by the presence of mush-room bodies belonging to older lineages exemplified here by *Lebbeus* belonging to the older infraorder Caridea, which originated from the ancestral decapod stem at the end of the Silurian (Porter et al., 2005). Stenopodidea, which like *Lebbeus* has mushroom bodies with columnar lobes (Wolff et al., 2017), originated even earlier at about 423 mya (Porter et al., 2005).

# 4.4 | Are only protocerebral elements of the crustacean olfactory system homologous with those of hexapods?

Does the presence of mushroom bodies in crustaceans suggest that their olfactory system is homologous to that of insects? This question has been the subject of considerable discussion and research, with the prevailing view that Crustacea and Hexapoda share the same ground pattern organization of their olfactory pathways and centers except for their olfactory association centers, which are considered analogues not homologues, the mushroom bodies being hexapod apomorphies (Harzsch & Krieger, 2018; Sandeman & Scholtz, 1995; Sandeman et al., 2014). Here, we argue that the available evidence suggests the opposite: that deutocerebral elements of insect and crustacean olfactory pathways do not obviously correspond, whereas their protocerebral components do.

Up to the present time, no crustacean species has been shown to possess odorant receptors (ORs) which typify those present in olfactory receptor neurons of dicondylic insects. [Correction added on 4 April 2019, after first online publication: the preceding sentence was modified.] In crustaceans, each olfactory sensillum, the aesthetasc, is populated by an abundance of olfactory receptor neuron dendrites, the responses of which are driven by ionotropic receptors (IRs) (Kozma et al., 2018). The same is observed in Archaeognatha, where also all olfactory receptor neurons are ionotropic (Groh-Lunow, Getahun, Grosse-Wilde, & Hansson, 2015; Missbach et al., 2014). In crustaceans, olfactory neuron axons do not appear to target specific olfactory lobe subunits although no definitive maps have been achieved relating the axons from populations of the same IR receptor neuron type to specific glomeruli. Generally, many thousands of axons from the olfactory receptor neurons reach the olfactory lobe with few or many terminals, depending on species, branching to invade single or several subunits (Harzsch & Krieger, 2018; Schmidt & Ache, 1992; Tuchina et al., 2015). This is a crucial distinction from insects, in which ligand-gated olfactory receptor neurons sort their axons centrally so that axons of each type of olfactory receptor neuron sort out to a specific glomerulus in the olfactory lobe to provide an odortypic map (Fishilevich & Vosshall, 2005). Consequently, in insects there are as many olfactory glomeruli as there are olfactory receptor neuron types, the exception being certain orthopterans in which receptor endings distribute to many microglomeruli (Ignell, Anton, & Hansson, 2001).

In insects, each glomerulus is served by 2–5 uniglomerular projection (relay) neurons, so-called because their dendrites are restricted to a single glomerulus. There is also a smaller population of multiglomerular projections, the dendrites of which extend to several or even all glomeruli. Bundled axons from projection neurons ascend to the lateral

protocerebrum on the same side of the brain (Galizia & Rössler, 2010). This arrangement contrasts with that of the crustacean olfactory lobe. Despite Hanström's imaginative depiction of the thalassinid *Calocaris macandreae* (Hanström, 1925), no crustacean, including thalassinids, has been shown to possess an arrangement of uniglomerular projection neurons, although some neurons provide dendrites that invade clusters of just a few glomeruli (Schmidt & Ache, 1996a, 1996b, 1997; Wachowiak & Ache, 1994). Instead, neurons relaying from the crustacean olfactory lobes have broad dendritic domains associated with very many of the lobe's subunits (Schmidt, 2016).

In insects, there may be as many as five uniglomerular projection neurons serving a glomerulus, which translates to 2-5 times more axons leaving an olfactory lobe as there are glomeruli comprising that lobe. In species of attine (harvester) ants equipped with over 600 antennal lobe glomeruli (Kelber, Rössler, Roces, & Kleineidam, 2009), there may be over 2.000 projection neuron axons. This is one extreme, the opposite being the pigeon louse where there are just three glomeruli and a corresponding paucity of outgoing axons (Crespo & Vickers, 2012). In eumalacostracan crustaceans, some thousands of olfactory lobe projection neurons provide ascending axons to the lateral protocerebrum. Generally, the OGTs carrying these axons from the two olfactory lobes meet at the midline of the protocerebrum where many of the axons bifurcate such that each lateral protocerebrum receives inputs from both olfactory lobes not just from the ipsilateral lobe as in insects. These differences between the insect and eumalacostracan (and the remipede) olfactory pathways in the deutocerebrum are profound. They become more so in the clade of decapod eumalacostracans known as Reptantia, which has evolved novel olfactory centers in the deutocerebrum called the paired accessory lobes (Sandeman & Scholtz, 1995). These receive no direct sensory input but are directly connected to the ipsilateral olfactory lobe and participate in ascending projections to the lateral protocerebrum and its hemiellipsoid bodies (Sullivan & Beltz, 2005). In Remipedia, determined by molecular phylogenetics as the sister of Hexapoda (Oakley et al., 2013; Regier et al., 2005), the deuto- and tritocerebra are organized according to the same distinctive ground pattern as in Eumalacostraca (Fanenbruck & Harzsch, 2005; Fanenbruck, Harzsch, & Wägele, 2004). In the remipede, a small satellite neuropil adjacent to its enormous olfactory lobes receiving no direct sensory inputs is distinctly glomerular like the accessory lobe of reptantians and is similarly connected to the olfactory lobe (see figures in Fanenbruck & Harzsch. 2005).

In short, other than the olfactory lobe's disposition in the deutocerebrum, no neuroanatomical arrangement identified in the crustacean olfactory system (including that of Remipedia) at the level of the deutocerebrum has been confidently resolved in a hexapod. Further distinctions relate to other neuropils in the deutocerebrum (and tritocerebrum) that have no counterpart in insects, and which are associated with the second antennae. Conversely, the evolved loss of the second antennae is reflected in a simplification of the insect tritocerebrum (Wolff & Strausfeld, 2015b).

In contrast to these many differences of olfactory pathway organization, corresponding distinctions do not appear to pertain to the protocerebrum, where insect and eumalacostracan genera possess phenotypically corresponding mushroom bodies or their evolved derivatives that lack columnar extensions, that is, the hemiellipsoid

bodies. One minor cause for confusion is that Stomatopoda and decapod Eumalacostraca also possess a second columnar neuropil in the lateral protocerebrum, called the reniform body, that serves the visual system in detecting and habituating to repetitive stimuli (Maza et al., 2016; Wolff et al., 2017). The correspondence of crustacean and insect protocerebra are also well supported with respect to the central complex neuropils and the protocerebrum's medial lobes (Thoen et al., 2017; Wolff et al., 2017). Other arrangements in the lateral protocerebra still await exploration. But, as demonstrated by Blaustein et al. (1988) and Sullivan and Beltz (2004), the lateral protocerebrum can no longer be viewed as a unitary region termed the medulla terminalis.

Homologies between insect and crustacean olfactory pathways are thus best attributed to the lateral protocerebrum and its corresponding second-order olfactory centers. This raises the question whether the extensive anatomical differences between the crustacean and insect deutocerebra, as outlined above, are due to divergent evolution or to evolved reduction and loss in Hexapoda. Demonstrating correspondences, if such exist, will depend on whether crustacean and insect deutocerebra share gene regulatory networks (character identity networks) that define common developmental patterns and identify corresponding morphologies in what may appear to be disparate morphological traits (see, Wagner, 2007). Demonstrating their shared genomic attributes may reconcile such differences as representing the "same organ in different animals under every variety of form and function," to quote Richard Owen's original definition of homology (Owen, 1843), bearing in mind Darwin's (1859) caveat that common ancestry is also required.

#### **ACKNOWLEDGMENTS**

The research described here is supported by the National Science Foundation under Grant No. 1754798 awarded to NJS. Support for animal collection was assisted by the University of Arizona's Center for Insect Science and the University of Arizona Regents' Fund. Our gratitude goes to the University of Washington's Friday Harbor Laboratory staff, as well as Billie Swalla, Bernadette Holthuis, and Meegan Corcoran, for their unfailing help in setting up research accommodation, piloting the trawls, and much invaluable advice. We thank Daniel Kalderon for supplying the DCO antibody: his generosity has been a major factor in this work and for other laboratories studying insect mushroom bodies. We have profited from discussions with Gabriella Wolff (University of Washington), Todd Oakley (University of California Santa Barbara), Hanne Thoen and Justin Marshall (Queensland Brain Institute), Greg Edgecombe (Natural History Museum, London), Gregory Jensen (University of Washington), and Charles Derby, (Georgia State University, Atlanta). We also thank Camilla Strausfeld for critically discussing and editing the text.

#### ORCID

Marcel E. Sayre https://orcid.org/0000-0002-2667-4228
Nicholas J. Strausfeld https://orcid.org/0000-0002-1115-1774

#### REFERENCES

- Andrew, D. R., Brown, S. M., & Strausfeld, N. J. (2012). The minute brain of the copepod *Tigriopus californicus* supports a complex ancestral ground pattern of the tetraconate cerebral nervous systems. *Journal of Comparative Neurology*, 520, 3446–3470. https://doi.org/10.1002/cne. 23099
- Antonsen, B. L., & Paul, D. H. (2001). Serotonergic and octopaminergic systems in the squat lobster *Munida quadrispina* (Anomura, Galatheidae). *Journal of Comparative Neurology*, 439, 450–468. https://doi.org/10.1002/cne.1362
- Aso, Y., Hattori, D., Yu, Y., Johnston, R. M., Iyer, N. A., Ngo, T. T., ... Rubin, G. M. (2014). The neuronal architecture of the mushroom body provides a logic for associative learning. *eLife*, 3, e04577. https://doi.org/10.7554/eLife.04577
- Bellonci, G. (1882). Nuove ricerche sulla struttura del ganglio ottico della Squilla mantis. Memorie della Accademia delle Scienze dell'Istituto di Bologna, 4, 419-426.
- Blaustein, D. N., Derby, C. D., Simmons, R. B., & Beall, A. C. (1988). Structure of the brain and medulla terminalis of the spiny lobster *Panulirus argus* and the crayfish *Procambarus clarkii*, with an emphasis on olfactory centers. *Journal of Crustacean Biology*, 8, 493–519. https://doi.org/10.2307/1548686
- Bodian, D. (1936). A new method for staining nerve fibers and nerve endings in mounted paraffin sections. *Anatomical Record*, *65*, 89–97. https://doi.org/10.1002/ar.1090650110
- Böhm, A., Szucsich, N. U., & Pass, G. (2012). Brain anatomy in Diplura (Hexapoda). Frontiers in Zoology, 9, 26. https://doi.org/10.1186/1742-9994-9-26
- Brauchle, M., Kiontke, K., MacMenamin, P., Fitch, D. H. A., & Piano, F. (2009). Evolution of early embryogenesis in rhabditid nematodes. Developmental Biology, 335, 253–262. https://doi.org/10.1016/j.ydbio. 2009 07 033
- Brown, S., & Wolff, G. (2012). Fine structural organization of the hemiellipsoid body of the land hermit crab, Coenobita clypeatus. Journal of Comparative Neurology, 520, 2847–2863. https://doi.org/10.1002/ cne 23058
- Cournil, I., Helluy, S. M., & Beltz, B. S. (1994). Dopamine in the lobster *Homarus gammarus*. I. Comparative analysis of dopamine and tyrosine hydroxylase immunoreactivities in the nervous system of the juvenile. *Journal of Comparative Neurology*, 334, 455–469. https://doi.org/10.1002/cne.903440308
- Crespo, J. G., & Vickers, N. J. (2012). Antennal lobe organization in the slender pigeon louse, *Columbicola columbae* (Phthiraptera: Ischnocera). *Arthropod Structure & Development*, 41, 227–230. https://doi.org/, https://doi.org/10.1016/j.asd.2012.02.008
- Crisp, K. M., Klukas, K. A., Gilchrist, L. S., Nartey, A. J., & Mesce, K. (2001). Distribution and development of dopamine- and octopaminesynthesizing neurons in the medicinal leech. *Journal of Comparative Neurology*, 442, 115–129. https://doi.org/, https://doi.org/10.1002/ cne.10077
- Crittenden, J. R., Skoulakis, E. M. C., Han, K.-A., Kalderon, D., & Davis, R. L. (1998). Tripartite mushroom body architecture revealed by antigenic markers. *Learning and Memory*, *5*, 38–51.
- Cronin, T. W., Caldwell, R. L., & Marshall, J. (2006). Learning in stomatopod crustaceans. *International Journal of Comparative Psychology*, 19, 297–317.
- Darwin, C. (1859). On the origin of species by means of natural selection, or the preservation of favoured races in the struggle for life. London, England: J. Murray.
- Derby, C., & Schmidt, M. (2017). *Crustacean olfaction*. Oxford research encyclopedia of neuroscience. New York: Oxford University Press.
- Duffy, J. E. (1996). Eusociality in a coral-reef shrimp. *Nature*, 381, 512-514. https://doi.org/10.1038/381512a0
- Fabricius, J. C. (1775). Systema entomologiae, sistens insectorum classes, ordines, genera, species, adjectis sysnonymis, locis, descriptionibus, observationibus (832 pp). Kortii: Flensburgi et Lipsiae.
- Fanenbruck, M., & Harzsch, S. (2005). A brain atlas of *Godzilliognomus* frondosus Yager, 1989 (Remipedia, Godzilliidae) and comparison with the brain of *Speleonectes tulumensis* Yager, 1987 (Remipedia, Speleonectidae): Implications for arthropod relationships. *Arthropod*

- Structure & Development, 34, 343-378. https://doi.org/10.1016/j. asd 2005.01.007
- Fanenbruck, M., Harzsch, S., & Wägele, J.W. (2004). The brain of the Remipedia (Crustacea) and an alternative hypothesis on their phylogenetic relationships. Proceedings of the National Academy of Sciences of the United States of America, 101, 3868–3873. https://doi.org/10. 1073/pnas.0306212101
- Farris, S. M. (2005). Evolution of insect mushroom bodies: Old clues, new insights. Arthropod Structure & Development, 34, 211–234. https://doi. org/10.1016/j.asd.2005.01.008
- Farris, S. M., & Schulmeister, S. (2011). Parasitoidism, not sociality, is associated with the evolution of elaborate mushroom bodies in the brains of hymenopteran insects. *Proceedings of the Royal Society B: Biological Sciences*, 278, 940–951. https://doi.org/10.1098/rspb.2010.2161
- Feder, H. M. (1966). Cleaning symbioses in the marine environment. In S. M. Henry (Ed.), Symbiosis (Vol. 1, pp. 327–380). New York, NY: Academic Press.
- Fishilevich, E., & Vosshall, L. B. (2005). Genetic and functional subdivision of the *Drosophila* antennal lobe. *Current Biology*, 15, 1548–1553. https://doi.org/, https://doi.org/10.1016/j.cub.2007.06.038
- Galizia, C. G., & Rössler, W. (2010). Parallel olfactory systems in insects: Anatomy and function. Annual Review of Entomology, 55, 399–420. https://doi.org/10.1146/annurev-ento-112408-085442
- Groh-Lunow, K. C., Getahun, M. N., Grosse-Wilde, E., & Hansson, B. S. (2015). Expression of ionotropic receptors in terrestrial hermit crab's olfactory sensory neurons. Frontiers in Cellular Neuroscience, 8, 448. https://doi.https://doi.org/10.3389/fncel.2014.00448
- Gronenberg, W., Heeren, S., & Hölldobler, B. (1996). Age-dependent and task-related morphological changes in the brain and the mushroom bodies of the ant Camponotus floridanus. Journal of Experimental Biology, 199, 2011–2019.
- Hamanaka, Y., Minoura, R., Nishino, H., Miura, T., & Mizunami, M. (2016). Dopamine- and tyrosine hydroxylase-immunoreactive neurons in the brain of the American cockroach, *Periplaneta americana*. *PLoS One*, 11, e0160531. https://doi.org/10.1371/journal.pone.0160531
- Hanström, B. (1925). The olfactory centers in crustaceans. *Journal of Comparative Neurology*, 38, 221–250. https://doi.org/10.1002/cne. 900380302
- Harzsch, S. (2004). Phylogenetic comparison of serotonin-immunoreactive neurons in representatives of the Chilopoda, Diplopoda, and Chelicerata: Implications for arthropod relationships. *Journal of Morphology*, 259, 198–213.
- Harzsch, S., Anger, K., & Dawirs, R. R. (1997). Immunocytochemical detection of acetylated α-tubulin and Drosophila synapsin in the embryonic crustacean nervous system. International Journal of Developmental Biology, 41, 477–484.
- Harzsch, S., & Hansson, B. S. (2008). Brain architecture in the terrestrial hermit crab *Coenobita clypeatus* (Anomura, Coenobitidae), a crustacean with a good aerial sense of smell. *BMC Neuroscience*, 9, 58. https://doi. org/10.1186/1471-2202-9-58
- Harzsch, S., & Krieger, J. (2018). Crustacean olfactory systems: A comparative review and a crustacean perspective on olfaction in insects. *Progress in Neurobiology*, 161, 23–60. https://doi.org/10.1016/j.pneurobio.2017. 11.005
- Harzsch, S., Rieger, V., Krieger, J., Seefluth, F., Strausfeld, N. J., & Hansson, B. S. (2011). Transition from marine to terrestrial ecologies: Changes in olfactory and tritocerebral neuropils in land-living isopods. Arthropod Structure & Development, 40, 244–257. https://doi.org/10. 1016/j.asd.2011.03.002
- Harzsch, S., & Waloszeck, D. (2000). Serotonin-immunoreactive neurons in the ventral nerve cord of Crustacea: A character to studyaspects of arthropod phylogeny. Arthropod Structure & Development, 29, 307–322. https://doi.org/10.1016/S1467-8039(01)00015-9
- Ignell, R., Anton, S., & Hansson, B. S. (2001). The antennal lobe of Orthoptera: Anatomy and evolution. *Brain, Behavior and Evolution, 57*, 1–17. https://doi.org/, https://doi.org/10.1159/000047222
- Ito, K., Shinomiya, K., Ito, M., Armstrong, J. D., Boyan, G., Hartenstein, V., ... Vosshall, L. B. (2014). A systematic nomenclature for the insect brain. *Neuron*, 81, 755–765. https://doi.org/10.1016/j.neuron.2013. 12.017

- Jensen, G. C. (1995). Pacific coast crabs and shrimps (p. 83). Montgomery, CA: Sea Challengers.
- Jensen, G. C. (2006). Three new species of *Lebbeus* (Crustacea: Decapoda: Hippolytidae) from the northeastern Pacific. *Zootaxa*, 1383, 23-43. https://doi.org/10.5281/zenodo.175047
- Kelber, C., Rössler, W., Roces, F., & Kleineidam, C. J. (2009). The antennal lobes of fungus-growing ants (attini): Neuroanatomical traits and evolutionary trends. *Brain, Behavior and Evolution*, 73, 273–284. https:// doi.org/10.1159/000230672
- Klagges, B. R., Heimbeck, G., Godenschwege, T. A., Hofbauer, A., Pflugfelder, G. O., Reifegerste, R., ... Buchner, E. (1996). Invertebrate synapsins: A single gene codes for several isoforms in *Drosophila. Jour*nal of Neuroscience, 16, 3154–3165.
- Kollmann, M., Huetteroth, W., & Schachtner, J. (2011). Brain organization in Collembola (springtails). Arthropod Structure & Development, 40, 304–316. doi:10.1016/j.asd.2011.02.003. https://doi.org/
- Komai, T. (2015). Reinstatement and redescription of *Lebbeus armatus* (Owen, 1839), long synonymized with *L. groenlandicus* (Fabricius, 1775), and description of one new species from the southwestern Sea of Okhotsk, Hokkaido, Japan (Crustacea: Decapoda: Caridea: Thoridae). *Zootaxa*, 3905, 451–473. doi:10.11646/zootaxa.3905.4.1. https://doi.org/
- Kozma, M. T., Schmidt, M., Ngo-Vu, H., Sparks, S. D., Senatore, A., & Derby, C. D. (2018). Chemoreceptor proteins in the Caribbean spiny lobster, *Panulirus argus*: Expression of ionotropic receptors, gustatory receptors, and TRP channels in two chemosensory organs and brain. *PLoS One*, 13, e0203935. https://doi.org/10.1371/journal.pone.0203935
- Lane, M. E., & Kalderon, D. (1993). Genetic investigation of cAMP-dependent protein-kinase function in *Drosophila* development. *Genes & Development*, 7, 1229–1243. doi:10.1101/gad.7.7a.1229. https://doi.org/
- Lange, A. B., & Chan, K. (2008). Dopaminergic control of foregut contractions in *Locusta migratoria*. *Journal of Insect Physiology*, 54, 222–230. https://doi.org/10.1016/j.jinsphys.2007.09.005
- Langeloh, H., Wasser, H., Richter, N., Bicker, G., & Stern, M. (2018). Neuromuscular transmitter candidates of a centipede (*Lithobius forficatus*, Chilopoda). Frontiers in Zoology, 15, 28. https://doi.org/10.1186/s12983-018-0274-9
- Limbaugh, C., Pederson, H., & Chase, F. (1961). Shrimps that clean fishes. Bulletin of Marine Science of the Gulf and Caribbean, 11, 237–257.
- Long, S. M. (2018). A novel protocol for generating intact, whole-head spider cephalothorax tissue sections. *BioTechniques*, 64, 163–169. https://doi.org/10.2144/btn-2018-2002
- Maza, F. J., Sztarker, J., Shkedy, A., Peszano, V. N., Locatelli, F. F., & Delorenzi, A. (2016). Context-dependent memory traces in the crab's mushroom bodies: Functional support for a common origin of high-order memory centers. Proceedings of the National Academy of Sciences of the United States of America, 113, E7957–E7965. https://doi.org/10.1073/pnas.1612418113
- McKinzie, M. E., Benton, J. J., Beltz, B. S., & Mellon, D. F. (2003). Parasol cells of the hemiellipsoid body in the crayfish *Procambarus clarkii*: Dendritic branching patterns and functional implications. *Journal of Comparative Neurology*, 462, 168–179. https://doi.org/10.1002/cne.10716
- Mellon, D. (2003). Active dendritic properties constrain input-output relationships in neurons of the central olfactory pathway in the crayfish forebrain. Microscopy Research and Technique, 60, 278–290. https://doi.org/10.1002/jemt.10267
- Mellon, D., Alones, V., & Lawrence, M. D. (1992). Anatomy and fine structure of neurons in the deutocerebral projection pathway of the cray-fish olfactory system. *Journal of Comparative Neurology*, 321, 93–111. https://doi.org/10.1002/cne.903210109
- Mellon, D. F., Jr. (2000). Convergence of multimodal sensory input onto higher-level neurons of the crayfish olfactory pathway. *Journal of Neu*rophysiology, 84, 3043–3055.
- Missbach, C., Dweck, H. K. M., Vogel, H., Vilcinskas, A., Stensmyr, M. C., Hansson, B. S., & Grosse-Wilde, E. (2014). Evolution of insect olfactory receptors. *eLife*, 3, e02115. https://doi.org/10.7554/eLife.02115
- Montgomery, S. H., Merrill, R. M., & Ott, S. R. (2016). Brain composition in Heliconius butterflies, posteclosion growth and experience-dependent neuropil plasticity. Journal of Comparative Neurology, 524, 1747–1769. https://doi.org/10.1002/cne.23993

- Mu, L., Ito, K., Bacon, J. P., & Strausfeld, N. J. (2012). Optic glomeruli and their inputs in *Drosophila* share an organizational ground pattern with the antennal lobes. *Journal of Neuroscience*, 32, 6061–6060. https://doi.org/10.1523/JNEUROSCI.0221-12.2012
- Nässel, D. R. (1988). Serotonin and serotonin-immunoreactive neurons in the nervous system of insects. *Progress in Neurobiology*, 30, 1–85.
- Nässel, D. R., & Elekes, K. (1992). Aminergic neurons in the brain of blowflies and *Drosophila*: Dopamine- and tyrosine hydroxylase-immunoreactive neurons and their relationship with putative histaminergic neurons. *Cell and Tis*sue Research, 267, 147–167. https://doi.org/10.1007/BF00318701
- Nässel, D. R., & Wegener, C. (2011). A comparative review of short and long neuropeptide F signaling in invertebrates: Any similarities to vertebrate neuropeptide Y signaling? *Peptides*, 32, 1335–1355. https:// doi.org/10.1016/j.peptides.2011.03.013
- Oakley, T. H., Wolfe, J. M., Lindgren, A. R., & Zaharoff, A. K. (2013). Phylotranscriptomics to bring the understudied into the fold: Monophyletic Ostracoda, fossil placement, and pancrustacean phylogeny. Molecular Biology and Evolution, 30, 215–233. https://doi.org/10.1093/molbev/mss216
- Owen, R. (1843). Lectures on the comparative anatomy and physiology of the invertebrate animals, delivered at the Royal College of Surgeons in 1843. London, England: Longman, Brown, Green and Longmans.
- Porter, M. L., Pérez-Losada, M., & Crandall, K. A. (2005). Model-based multi-locus estimation of decapod phylogeny and divergence times. Molecular Phylogenetics and Evolution, 37, 355–369.
- Regier, J. C., Shultz, J. W., & Kambic, R. E. (2005). Pancrustacean phylogeny: Hexapods are terrestrial crustaceans and maxillopods are not monophyletic. *Proceedings of the Royal Society B: Biological Sciences*, 272, 395–401. https://doi.org/10.1098/rspb.2004.2917
- Sandeman, D. C., Kenning, M., & Harzsch, S. (2014). Adaptive trends in malacostracan brain form and function related to behavior. In C. D. Derby & M. Thiel (Eds.), *The natural history of the Crustacea* (Vol. 3. pp. 11–48). Oxford. England: Oxford University Press.
- Sandeman, D. C., & Scholtz, G. (1995). Ground plans, evolutionary changes and homologies in decapod crustacean brains. In O. Breidbach & W. Kutsch (Eds.), The nervous systems of invertebrates: An evolutionary and comparative approach (pp. 329–347). Basel, Switzerland: Birkhäuser Verlag.
- Schindelin, J., Arganda-Carreras, I., Frise, E., Kaynig, V., Longair, M., Pietzsch, T., ... Cardona, A. (2012). Fiji: An open-source platform for biological-image analysis. *Nature Methods*, 9, 676–682. https://doi. org/10.1038/NMETH.2019
- Schmidt, M. (2016). Malacostraca. In A. Schmidt-Rhaesa, S. Harzsch, & G. Purschke (Eds.), Structure & evolution of invertebrate nervous systems (pp. 529–582). Oxford, England: Oxford University Press.
- Schmidt, M., & Ache, B. W. (1992). Antennular projections to the midbrain of the spiny lobster. II. Sensory innervation of the olfactory lobe. *Journal of Comparative Neurology*, 318, 291–303. https://doi.org/10.1002/cne.903180306
- Schmidt, M., & Ache, B. W. (1996a). Processing of antennular input in the brain of the spiny lobster, *Panulirus argus*. I. Non-olfactory chemosensory and mechanosensory pathway of the lateral and median antennular neuropils. *Journal of Comparative Physiology A*, 178, 579–604. https://doi.org/10.1007/BF00227375
- Schmidt, M., & Ache, B. W. (1996b). Processing of antennular input in the brain of the spiny lobster, *Panulirus argus*. II. The olfactory pathway. *Journal of Comparative Physiology A*, 178, 605–628. https://doi.org/10. 1007/BF00227374
- Schmidt, M., & Ache, B. W. (1997). Immunocytochemical analysis of glomerular regionalization and neuronal diversity in the olfactory deutocerebrum of the spiny lobster. *Cell and Tissue Research*, 287, 541–563. https://doi.org/10.1007/s004410050778
- Schwentner, M., Richter, S., Rogers, D. C., & Giribet, G. (2018). Tetraconatan phylogeny with special focus on Malacostraca and Branchiopoda: Highlighting the strength of taxon-specific matrices in phylogenomics. *Proceedings of the Royal Society B: Biological Sciences*, 285, 20181524. https://doi.org/10.1098/rspb.2018.1524
- Skoulakis, E. M. C., Kalderon, D., & Davis, R. L. (1993). Preferential expression in mushroom bodies of the catalytic subunit of protein kinase A and its role in learning and memory. *Neuron*, 11, 197–208. https://doi.org/10.1016/0896-6273(93)90178-T

- Stegner, M. E., & Richter, S. (2011). Morphology of the brain in *Hutchinsoniella macracantha* (Cephalocarida, Crustacea). *Arthropod Structure & Development*, 40, 221–243. https://doi.org/10.1016/j.asd. 2011.04.001
- Stegner, M. E. J., Stemme, T., Iliffe, T. M., Richter, S., & Wirkner, C. S. (2015). The brain in three crustaceans from cavernous darkness. BMC Neuroscience, 16, 19. https://doi.org/10.1186/s12868-015-0138-6
- Stemme, R., Eickhoff, R., & Bicker, G. (2014). Olfactory projection neuron pathways in two species of marine Isopoda (Peracarida, Malacostraca, Crustacea). *Tissue and Cell*, 46, 260–263. https://doi.org/10.1016/j. tice.2014.05.010
- Stemme, T., Iliffe, T. M., & Bicker, G. (2016). Olfactory pathway in *Xibalbanus tulumensis*: Remipedian hemiellipsoid body as homologue of hexapod mushroom body. *Cell and Tissue Research*, *363*, 635–648. https://doi.org/10.1007/s00441-015-2275-8
- Stern, M. (2009). The PM1 neurons, movement sensitive centrifugal visual brain neurons in the locust: Anatomy, physiology, and modulation by identified octopaminergic neurons. *Journal of Comparative Physiology* A. Sensory Neural and Behavioral Physiology, 195, 123–137. https://doi. org/, https://doi.org/10.1007/s00359-008-0392-5
- Strausfeld, N. J. (2018). The divergent evolution of arthropod brains: Ground pattern organization and stability through geological time. In J. H. Byrne (Ed.), *The Oxford handbook of invertebrate neurobiology*, New York: Oxford University Press.
- Strausfeld, N. J., & Li, Y. (1999). Organization of olfactory and multimodal afferent neurons supplying the calyx and pedunculus of the cockroach mushroom bodies. *Journal of Comparative Neurology*, 409, 603–625. https://doi.org/10.1002/(SICI)1096-9861(19990712)409:4<603::AID-CNE7>3.0.CO;2-P
- Strausfeld, N. J., & Meinertzhagen, I. A. (1998). The insect neuron: Morphologies, structures and relationships to neuroarchitecture. In F. W. Harrison & M. Locke (Eds.), Microscopic anatomy of invertebrates (Vol. 11b, pp. 487–538). New York, NY: Wiley-Liss.
- Strausfeld, N. J., Sinakevitch, I., Brown, S. M., & Farris, S. M. (2009). Ground plan of the insect mushroom body: Functional and evolutionary implications. *Journal of Comparative Neurology*, 513, 265–291. https://doi.org/10.1002/cne.21948
- Strausfeld, N. J., Strausfeld, C. M., Stowe, S., Rowell, D., & Loesel, R. (2006). The organization and evolutionary implications of neuropils and their neurons in the brain of the onychophoran *Euperipatoides rowelli*. Arthropod Structure & Development, 35, 169–196. https://doi.org/10.1016/j.asd.2006.06.002
- Sullivan, J. M., & Beltz, B. S. (2004). Evolutionary changes in the olfactory projection neuron pathways of eumalacostracan crustaceans. *Journal* of Comparative Neurology, 470, 25–38. https://doi.org/10.1002/cne. 11026
- Sullivan, J. M., & Beltz, B. S. (2005). Integration and segregation of inputs to higher-order neuropils of the crayfish brain. *Journal of Comparative Neurology*, 481, 118–126. https://doi.org/10.1016/j.asd. 2006.06.002
- Sullivan, J. M., Benton, J. L., Sandeman, D. C., & Beltz, B. S. (2007). Adult neurogenesis: A common strategy across diverse species. *Journal of Comparative Neurology*, 500, 574–584. https://doi.org/10.1002/cne. 21187
- Thazhath, R., Liu, C., & Gaertig, J. (2002). Polyglycylation domain of β-tubulin maintains axonemal architecture and affects cytokinesis in *Tetrahymena*. *Nature Cell Biology*, *4*, 256–259. https://doi.org/, https://doi.org/10.1038/ncb764
- Thoen, H. H., Marshall, J., Wolff, G. H., & Strausfeld, N. J. (2017). Insect-like organization of the stomatopod central complex: Functional and phylogenetic implications. Frontiers in Behavioral Neuroscience, 11, 12. https://doi.org/10.3389/fnbeh.2017.00
- Trivers, R. L. (1971). The evolution of reciprocal altruism. *Quarterly Review of Biology*, 46, 35–57. https://doi.org/10.1086/406755
- Tuchina, O., Koczan, S., Harzsch, S., Rybak, J., Wolff, G., Strausfeld, N. J., & Hansson, B. S. (2015). Central projections of antennular chemosensory and mechanosensory afferents in the brain of the terrestrial hermit crab (*Coenobita clypeatus*; Coenobitidae, Anomura). Frontiers in Neuroanatomy, 9, 94. https://doi.org/10.3389/fnana.2015. 00094

RESEARCH IN STSTEMS ABURDOSCIENCE \_\_WILE\_

Ebersberger, I., ... Misof, B. (2012). Pancrustacean phylogeny in the light of new phylogenomic data: Support for Remipedia as the possible sister group of hexapoda. Molecular Biology and Evolution, 29, 1031-1045. https://doi.org/10.1093/molbev/msr270

von Reumont, B. M., Jenner, R. A., Wills, M. A., Dell'ampio, E., Pass, G.,

- Wachowiak, M., & Ache, B. W. (1994). Morphology and physiology of multiglomerular olfactory projection neurons in the spiny lobster. Journal of Compararive Physiology A, 175, 35-48.
- Wagner, G. P. (2007). The developmental genetics of homology. Nature Reviews Genetics, 8, 473-479. https://doi.org/10.1038/nrg2099
- Withers, G. S., Day, N. F., Talbot, E. F., Dobson, H. E. M., & Wallace, C. S. (2008). Experience-dependent plasticity in the mushroom bodies of the solitary bee Osmia lignara (Megachilidae). Developmental Neurobiologv. 68, 73-82, https://doi.org/10.1002/dneu.20574
- Wolff, G., Harzsch, S., Hansson, B. S., Brown, S., & Strausfeld, N. J. (2012). Neuronal organization of the hemiellipsoid body of the land hermit crab, Coenobita clypeatus: Correspondence with the mushroom body ground pattern. Journal of Comparative Neurology, 520, 2824-2846. https://doi.org/10.1002/cne.23059

- Wolff, G. H., & Strausfeld, N. J. (2015a). Genealogical correspondence of mushroom bodies across invertebrate phyla. Current Biology, 25. 38-44. https://doi.org/10.1016/j.cub.2014.10.049
- Wolff, G. H., & Strausfeld, N. J. (2015b). The insect brain: A commentated primer. In A. Schmidt-Rhaesa, S. Harzsch, & G. Purschke (Eds.), Structure and evolution of invertebrate nervous systems (pp. 597-639). Oxford, England: Oxford University Press.
- Wolff, G. H., Thoen, H. H., Marshall, J., Savre, M. E., & Strausfeld, N. J. (2017). An insect-like mushroom body in a crustacean brain. eLife, 6, e29889. https://doi.org/10.7554/eLife.29889

How to cite this article: Sayre ME, Strausfeld NJ. Mushroom bodies in crustaceans: Insect-like organization in the caridid shrimp Lebbeus groenlandicus. J Comp Neurol. 2019;527: 2371-2387. https://doi.org/10.1002/cne.24678